Available online at www.sciencedirect.com

SciVerse ScienceDirect

Ceramics International 39 (2013) 331–336

CERAMICS INTERNATIONAL

www.elsevier.com/locate/ceramint

Electrochemical properties of nanometer-sized $0.6Li_2MnO_3 \cdot 0.4LiNi_{0.5}Mn_{0.5}O_2$ composite powders prepared by flame spray pyrolysis

Jung Hyun Kim, Seung Ho Choi, Mun Yeong Son, Min Ho Kim, Jung-Kul Lee, Yun Chan Kang*

Department of Chemical Engineering, Konkuk University, 1 Hwayang-dong, Gwangjin-gu, Seoul 143-701, Republic of Korea

Received 6 April 2012; received in revised form 31 May 2012; accepted 8 June 2012
Available online 19 June 2012

Abstract

Nanometer-sized $0.6Li_2MnO_3 \cdot 0.4LiNi_{0.5}Mn_{0.5}O_2$ composite cathode powders are prepared directly by high-temperature flame spray pyrolysis. The precursor powders and the powders post-treated at 800 °C exhibit mixed-layered crystal structures comprising layered Li_2MnO_3 and layered $LiNi_{0.5}Mn_{0.5}O_2$ phases. The discharge capacity of the precursor powders decreased from 193 mAh g^{-1} to 96 mAh g^{-1} by the 9th cycle, corresponding to a capacity retention of 49.7%. Post-treatment at 800 °C increases the capacity retention of the post-treated composite powders to 94.6% after 50 cycles, corresponding to a decrease in the discharge capacity from 225 to 213 mAh g^{-1}. The post-treated composite powders that contain a high amount of the Li_2MnO_3 phase have a high initial discharge capacity and good cyclability.

Keywords: Cathode material; Spray pyrolysis; Composite; Nanopowders

1. Introduction

The electrochemical performance of the cathode in the lithium ion secondary battery is affected by the properties of the cathode powders such as morphology, mean size, specific surface area, crystallinity and composition [1–4]. Improved electrochemical performance of the cathode may be derived from rapid Li^+ ion diffusion. An effective means of enhancing the rate of Li^+ diffusion in the cathode is to utilize nanomaterials [5]. Nanosized cathode powders provide a short diffusion length and more active surface area for Li^+ intercalation [6]. Recently, Li_2MnO_3-stabilized cathodes with composite structures have become attention due to their high capacity of over 200 mAh g^{-1} and enhanced safety at voltages exceeding 4.5 V [7–20]. The preparation of nanometer-sized Li_2MnO_3-stabilized electrodes has been achieved using various techniques. Kim et al. prepared composite of Li_2MnO_3 and $LiNi_{0.5}Mn_{0.3}Co_{0.2}O_2$ as nanostructural cathode materials using a high-energy ball milling method [10]. The particle diameters of the nanostructure electrodes prepared by the ball milling process were significantly smaller than those of bulk-type electrodes. Feng et al. synthesized a $Li[Ni_{0.2}Li_{0.2}Mn_{0.6}]O_2$ composite by using the "mixed oxalate" method, in which a homogeneous mixed oxalate of NiC_2O_4 and MnC_2O_4 obtained from oxalate co-precipitation was used as the precursor [11]. Subsequent heat-treatment of the mixture containing the precursor and $LiNO_3$ produced the highly electrochemically active $Li[Ni_{0.2}Li_{0.2}Mn_{0.6}]O_2$.

Flame spray pyrolysis is technique widely used to synthesize a number of functional powders over sizes ranging from nanometers to micrometers. Flame spray pyrolysis has been used in the synthesis of aggregation-free nanocathode powders [21–23].

*Corresponding author. Tel.: +82 2 2049 6010; fax: +82 2458 3504.
E-mail address:
lobat.tayebi@okstate.edu (Y.C. Kang).

0272-8842/$36.00
http://dx.doi.org/10.1016/j.ceramint.2012.06.029

In this study, the physical and electrochemical properties of nanometer-sized $0.6Li_2MnO_3 \cdot 0.4LiNi_{0.5}Mn_{0.5}O_2$ composite cathode powders prepared by high-temperature flame spray pyrolysis using an aqueous spray solution of metal salts are investigated.

2. Experimental

$0.6Li_2MnO_3 \cdot 0.4LiNi_{0.5}Mn_{0.5}O_2$, or equivalently $Li[Li_{0.2}Ni_{0.2}Mn_{0.6}]O_2$, composite cathode powders were prepared directly by high-temperature flame spray pyrolysis. The system consists of a droplet generator, a flame nozzle, a quartz reactor, a powder collector, and a blower [20]. Propane (fuel) and oxygen (oxidizer) were used to produce the diffusion flame. The flow rate of the fuel gas was 5 L min^{-1}. The flow rates of the oxidizer and carrier gases were fixed at 40 L min^{-1} and 10 L min^{-1}, respectively. A 1.7-MHz ultrasonic spray generator with six resonators was used to generate the droplets, which were then carried into the high-temperature diffusion flame by oxygen carrier gas. A mixed solvent with a volume ratio of ethyl alcohol to distilled water of 3:7 was used to produce a solution with an overall concentration of lithium, nickel and manganese components of 0.5 M. The starting materials used for the synthesis were $LiNO_3$ (Junsei, 98%), $Ni(NO_3)_2 \cdot 6H_2O$ (Junsei, 98%), and $Mn(CH_3COO) \cdot 4H_2O$ (Junsei, 97%). The amount of excess lithium in the solution was 15% of the stoichiometric amount. To improve the crystallinity and remove possible impurity-phases, the as-prepared powders obtained by flame spray pyrolysis were post-treated in a box furnace at 800 °C for 12 h.

The crystal structures of the precursor and composite powders were investigated using X-ray diffractometry (XRD, Rigaku DMAX-33) using Cu Kα radiation at room temperature in the 2θ range of 16–80°. The morphological characteristics of the powders were evaluated using scanning electron microscopy (SEM, JEOL, JSM-6060) and transmission electron microscopy (TEM, JEOL, JEM-2010). An electrode was fabricated using a mixture of 12 mg of the composite powders and 4 mg of TAB (TAB is a mixture of 3.2 mg of teflonized acetylene black and 0.8 mg of a binder). Lithium metal and a microporous polypropylene film were used as the counter electrode and separator, respectively. The electrolyte (TECHNO Semichem Co.) was 1 M $LiPF_6$ in a 1:1 (v/v) mixture of EC/DMC. The entire cell was assembled in a glove box under argon atmosphere. The charge/discharge characteristics of the samples were determined by potential cycling in the range of 2.5–4.8 V at a constant current of 20 mA g^{-1}.

3. Results and discussion

The morphologies of the precursor powders prepared directly by flame spray pyrolysis are shown in the SEM and TEM images in Fig. 1. The intermediate powders formed from the several microns droplets by drying and decomposition processes completely evaporated to the vapors of Li, Ni and Mn components inside the high temperature diffusion flame. Consequently, nanometer-sized precursor powders were formed from the vapors by nucleation and growth processes. No micron or submicron-sized particles directly prepared from the droplets were observed in the SEM image. The precursor powders, as shown in the TEM image, had a broad size distribution, and cubic and hexagonal morphology.

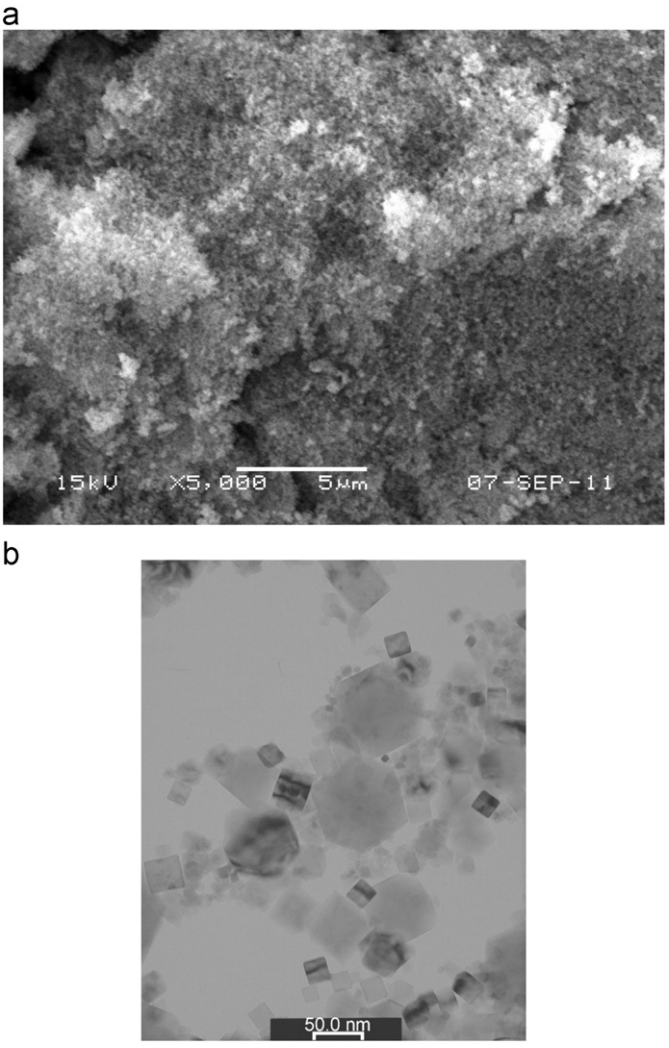

Fig. 1. SEM and TEM images of the precursor powders prepared by flame spray pyrolysis. (a) SEM image and (b) TEM image.

The precursor powders obtained by flame spray pyrolysis were post-treated in the box furnace at 800 °C, to improve the physical and electrochemical properties. XRD patterns of the precursor and post-treated powders are shown in Fig. 2. All of the peaks of the precursor and post-treated powders can be indexed based on a hexagonal α-$NaFeO_2$ structure, except for the peak near 21°, which is attributed to the superlattice structure of Li_2MnO_3 [12–14]. The precursor and post-treated powders had mixed-layered crystal structures consisting of layered Li_2MnO_3 and layered $LiNi_{0.5}Mn_{0.5}O_2$ phases and formed a

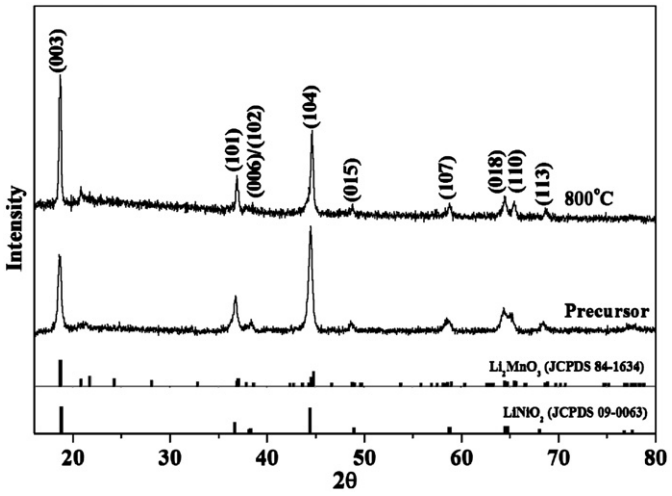

Fig. 2. XRD patterns of the precursor and post-treated $0.6Li_2MnO_3 \cdot 0.4LiNi_{0.5}Mn_{0.5}O_2$ composite powders.

composite compound. The precursor powders prepared directly by flame spray pyrolysis had broad and low intensity XRD peaks because of low crystallinity due to the short residence time of the composite powders inside the high-temperature diffusion flame. Post-treatment of the precursor powders resulted in sharper XRD peaks and increased intensity of the peak corresponding to the layered Li_2MnO_3 phase. The $I_{(003)}/I_{(104)}$ intensity ratio in the XRD pattern has been proposed to be a critical indicator of the degree of the anti-site mixing of Ni and Li [24–26]. The $I_{(003)}/I_{(104)}$ intensity ratio of the precursor powders is less than 1. In contrast, the $I_{(003)}/I_{(104)}$ ratio of the post-treated cathode powders was greater than 1. The clear (018)/(110) peak split is also indicative of the highly crystalline layered structure of the post-treated composite powders.

Fig. 3 shows the SEM and TEM images of the post-treated $0.6Li_2MnO_3 \cdot 0.4LiNi_{0.5}Mn_{0.5}O_2$ composite powders. The post-treated composite powders consist of nanometer-sized particles and had a slightly aggregated morphology. When the two solid phases are mixed, each phase prevents the crystal growth of the other phase. As a result, the composite powders had nanometer sizes even after post-treatment at the high temperature of 800 °C.

Figs. 4 and 5 show the initial charge-discharge curves and differential capacity vs. voltage (dQ/dV) curves of the precursor and post-treated composite powders at a constant current density of 20 mA g^{-1} in the range from 2.0 to 4.8 V at room temperature. Two distinct electrochemical reactions were observed in the initial charge curves of the post-treated composite powders. The smoothly sloping voltage profile below 4.5 V in Fig. 4 is due to the removal of Li from the $LiNi_{0.5}Mn_{0.5}O_2$ component [16–18]. The voltage plateau above 4.5 V is attributed to the removal of Li_2O from the Li_2MnO_3 component [12,19]. The voltage plateau at around 4.7 V in the initial charge curve corresponds to the sharp oxidation peak in the dQ/dV curve shown in Fig. 5. A small oxidation peak at around

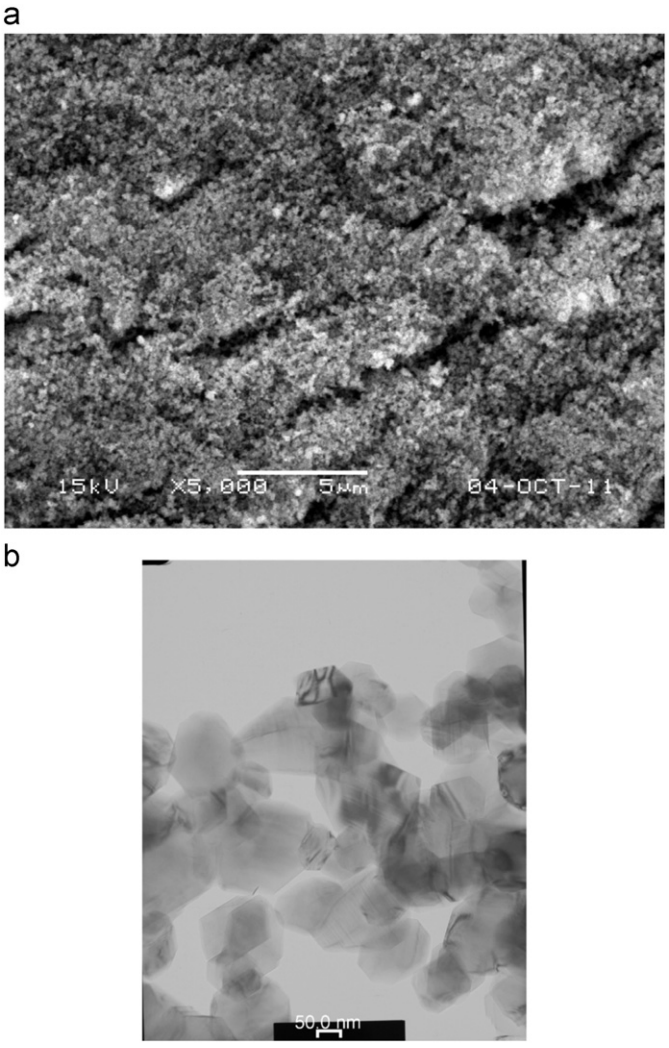

Fig. 3. SEM and TEM images of the $0.6Li_2MnO_3 \cdot 0.4LiNi_{0.5}Mn_{0.5}O_2$ composite powders post-treated at 800 °C. (a) SEM image and (b) TEM image.

3.7 V was also observed in the dQ/dV curve of the post-treated composite powders, due to the oxidation of Ni ions of the $LiNi_{0.5}Mn_{0.5}O_2$ component. The initial charge curve of the precursor composite powders had two voltage plateaus at around 4.3 V and 4.7 V. Two oxidation peaks at around 4.3 V and 4.7 V were also observed in the dQ/dV curve of the precursor composite powders. The voltage plateau and oxidation peak at around 4.7 V in Figs. 4 and 5 were attributed to the removal of Li_2O from the Li_2MnO_3 component. The voltage plateau at around 4.3 V was observed only in the precursor composite powders. In the previous report, the plateau at around 4.3 V was observed at around $x = 0.6$–0.7 $[Li_{1-x}(Ni_{0.5}Mn_{0.5})O_2]$ [27]. The precursor and post-treated composite powders had similar initial discharge curves. Two reduction peaks were present in the dQ/dV curves at around 3.3 and 3.8 V, corresponding to the $Mn^{4+}/^{3+}$ and $Ni^{4+}/^{2+}$ reductions, respectively [28,29]. The initial charge and discharge capacities of the precursor composite powders were 265 and 192 mAh g^{-1}, respectively. However, the initial charge and discharge capacities of the

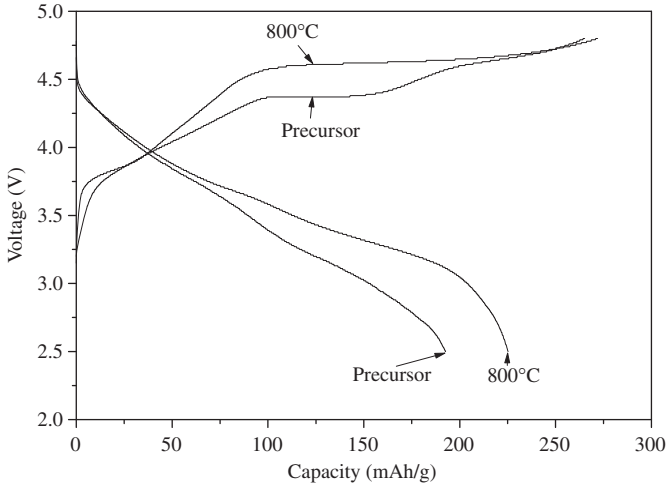

Fig. 4. Initial charge/discharge curves of the precursor and post-treated $0.6Li_2MnO_3 \cdot 0.4LiNi_{0.5}Mn_{0.5}O_2$ composite powders.

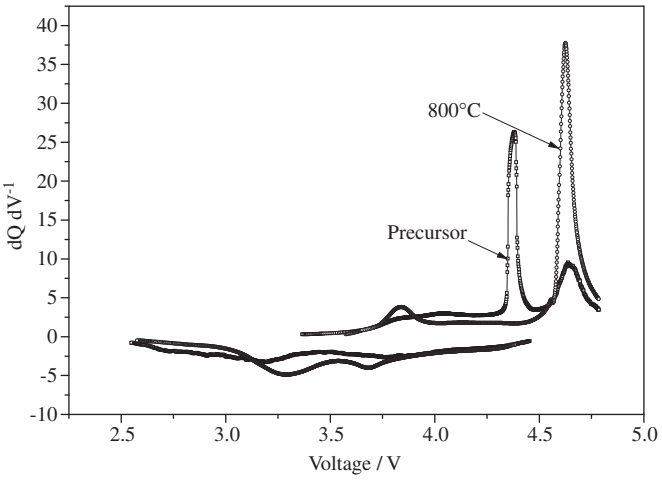

Fig. 5. Differential capacity vs. voltage (dQ/dV) of the precursor and post-treated $0.6Li_2MnO_3 \cdot 0.4LiNi_{0.5}Mn_{0.5}O_2$ composite powders.

post-treated composite powders were 272 and 225 mAh g^{-1}, respectively. The Coulombic efficiencies of the first cycles of the precursor and post-treated composite powders were 72.5 and 82.7% respectively.

Fig. 6 shows the cycle properties of the precursor and post-treated $0.6Li_2MnO_3 \cdot 0.4LiNi_{0.5}Mn_{0.5}O_2$ composite powders at a constant current density of 20 mA g^{-1} in the range from 2.0 to 4.8 V. The discharge capacity of the post-treated composite powders decreased from 225 to 213 mAh g^{-1} after 50 cycles, corresponding to a capacity retention of 94.6%. The layered $LiNi_{0.5}Mn_{0.5}O_2$ cathode material generally exhibits poor cycle performance at operating voltages above 4.5 V [30,31]. However, the composite powders exhibited good cycle performance even at high operating voltages due to the improved structural stability derived from the formation of Li_2MnO_3 [7–20]. In contrast, the precursor powders had poor cycle performance. The discharge capacity of the precursor composite powders decreased from 193 mAh g^{-1} to 96 mAh g^{-1} by

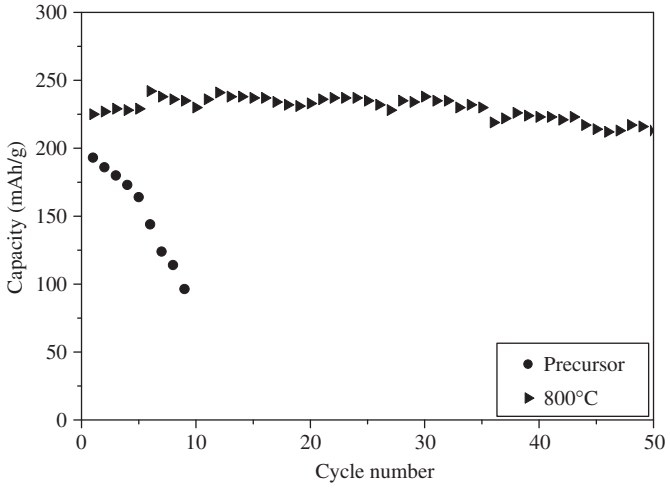

Fig. 6. Cycle properties of the precursor and post-treated $0.6Li_2MnO_3 \cdot 0.4LiNi_{0.5}Mn_{0.5}O_2$ composite powders.

the 9th cycle, corresponding to a capacity retention of 49.7%. The precursor composite powders prepared directly by flame spray pyrolysis contained only a small amount of layered Li_2MnO_3 material. Therefore, the structural stability derived from the formation of Li_2MnO_3 was not imparted to the precursor composite powders. The poor cycle property was also due to the high surface area and low crystallinity of the precursor powders. The cycle performance of the post-treated composite powders, indicated by the discharge capacities of the powders, gradually increases until the 5th cycle. This increase in the capacity with successive cycles can be explained by considering the dQ/dV curves shown in Fig. 7. The intense oxidation peak at around 4.7 V in the first charge curve disappeared in the subsequent cycles. MnO_2 formed from Li_2MnO_3 by elimination of Li_2O in the initial charge process is gradually transformed into layered $LiMnO_2$ with progressive cycles [9]. Therefore, the discharge capacities of the post-treated composite powders increase until the 5th cycle. The reduction peaks in the dQ/dV curves shifted to the low-voltage region as the cycle number increased. The dQ/dV curve of the 50th cycle had a main reduction peak at around 2.8 V. Reduction peaks below 3.0 V are attributed to the spinel $LiMn_2O_4$ phase. Thus, it can be deduced that the layered $LiMnO_2$ phase transformed to the spinel-like phases during charge/discharge cycling [32].

4. Conclusions

Nanometer-sized composite powders of $0.6Li_2MnO_3 \cdot 0.4LiNi_{0.5}Mn_{0.5}O_2$, with two solid phases, were synthesized directly by high-temperature flame spray pyrolysis. Due to mutual suppression of the crystal growth of one phase by the other, the composites exhibited an only slightly aggregated morphology even after post-treatment at 800 °C. The first cycle dQ/dV curve of the post-treated composite powders exhibits an intense oxidation peak at around 4.7 V, which is attributed to the removal of Li_2O

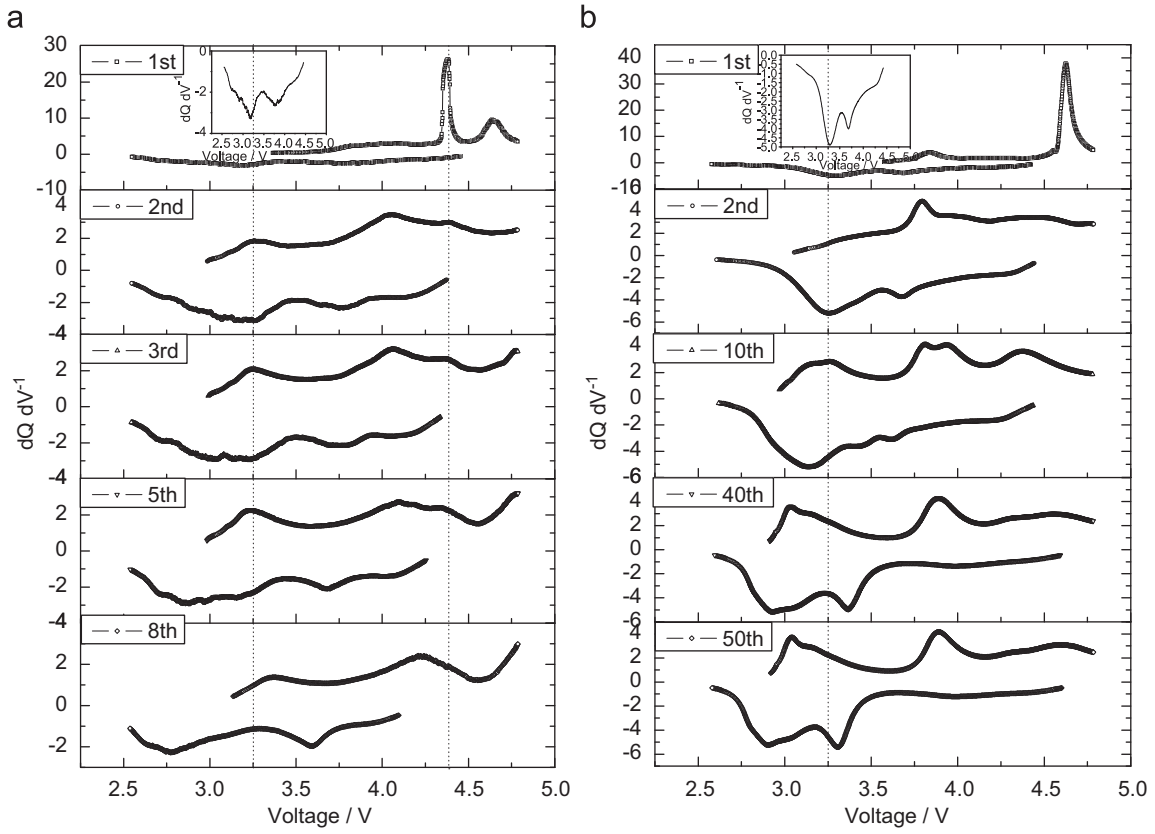

Fig. 7. Differential capacity vs. voltage (dQ/dV) of the precursor and post-treated $0.6Li_2MnO_3 \cdot 0.4LiNi_{0.5}Mn_{0.5}O_2$ composite powders according to the cycle numbers. (a) Precursor and (b) 800°C.

from the Li_2MnO_3 component. However, the first cycle dQ/dV curve of the precursor composite powders is characterized by an intense oxidation peak at around 4.3 V. The precursor composite powders prepared directly by flame spray pyrolysis containing only a small amount of layered Li_2MnO_3 material show poor electrochemical properties. In contrast, the electrochemical properties of the post-treated composite powders were improved at a high operating voltage relative to the precursors due to the structural stability derived from the Li_2MnO_3 phase.

Acknowledgment

This study was supported by the Converging Research Center Program through the National Research Foundation of Korea (NRF) funded by the Ministry of Education, Science and Technology (2011-50210).

References

[1] S.H. Ju, Y.C. Kang, Fine-sized $LiNi_{0.8}Co_{0.15}Mn_{0.05}O_2$ cathode particles prepared by spray pyrolysis from the polymeric precursor solutions, Ceramics International 35 (2009) 1633.

[2] J. Xie, X. Huang, Z. Zhu, J. Dai, Hydrothermal synthesis of $LiNi_xCo_{1-x}O_2$ cathode materials, Ceramics International 37 (2011) 665.

[3] B. Lin, Z. Wen, Z. Gu, S. Huang, Morphology and electrochemical performance of $Li[Ni_{1/3}Co_{1/3}Mn_{1/3}]O_2$ cathode material by a slurry spray drying method, Journal of Power Sources 175 (2008) 564.

[4] T. Ogihara, H. Aikiyo, N. Ogata, K. Katayama, Y. Azuma, H. Okabe, T. Okawa, Particle morphology and battery properties of lithium manganate synthesized by ultrasonic spray pyrolysis, Advanced Powder Technology 13 (2002) 437.

[5] K.M. Begam, S.R.S. Prabaharan, Improved cycling performance of nano-composite $Li_2Ni_2(MoO_4)_3$ as a lithium battery cathode material, Journal of Power Sources 159 (2006) 319.

[6] Y.J. Wei, K. Nikolowski, S.Y. Zhan, H. Ehrenberg, S. Oswald, G. Chen, C.Z. Wang, H. Chen, Electrochemical kinetics and cycling performance of nano $Li[Li_{0.23}Co_{0.3}Mn_{0.47}]O_2$ cathode material for lithium ion batteries, Electrochemistry communications 11 (2009) 2008.

[7] Z. Lu, D.D. MacNeil, J.R. Dahn, Layered cathode materials $Li[Ni_xLi_{(1/3-2x/3)}Mn_{(2/3-x/3)}]O_2$ for lithium-ion batteries, Electrochemical and Solid State Letters 4 (2001) 191.

[8] J.H. Kim, C.S. Yoon, Y.K. Sun, Structural characterization of $Li[Li_{0.1}Ni_{0.35}Mn_{0.55}]O_2$ cathode material for lithium secondary batteries, Journal of the Electrochemical Society 150 (2003) 538.

[9] Z. Lu, J.R. Dahn, Understanding the anomalous capacity of $Li/Li[Ni_xLi_{(1/3-2x/3)}Mn_{(2/3-x/3)}]O_2$ cells using in situ X-ray diffraction and electrochemical studies, Journal of the Electrochemical Society 149 (2002) 815.

[10] S.B. Kim, S.J. Kim, C.H. Kim, W.S. Kim, K.W. Park, Nanostructure cathode materials prepared by high-energy ball milling method, Materials Letters 65 (2011) 3313.

[11] F. Wu, H. Lu, Y. Su, N. Li, L. Bao, S. Chen, Preparation and electrochemical performance of Li-rich layered cathode material, $Li[Ni_{0.2}Li_{0.2}Mn_{0.6}]O_2$, for lithium-ion batteries, Journal of Applied Electrochemistry 40 (2010) 783.

[12] Z. Lu, L.Y. Beaulieu, A. Donaberger, C.L. Thomas, J.R. Dahn, Synthesis, structure, and electrochemical behavior of $Li[Ni_x Li_{1/3-2x/3}Mn_{2/3-x/3}]O_2$, Journal of the Electrochemical Society 149 (2002) 778.

[13] M.M. Thackeray, S.H. Kang, C.S. Johnson, J.T. Vaughey, R. Benedek, S.A. Hackney, Li_2MnO_3-stabilized $LiMO_2$ (M=Mn, Ni, Co) electrodes for lithium-ion batteries, Journal of Materials Chemistry 17 (2007) 3112.

[14] Z. Lu, Z. Chen, J.R. Dahn, Lack of cation clustering in $Li[Ni_x Li_{1/3-2x/3}Mn_{2/3-x/3}]O_2$ $(0 < x \leq 1/2)$ and $Li[Cr_x Li_{(1-x)/3}Mn_{(2-2x)/3}]O_2$ $(0 < x < 1)$, Chemistry of Materials 15 (2003) 3214.

[15] A. Pramanik, C. Ghanty, S.B. Majumder, Synthesis and electrochemical characterization of $xLi(Ni_{0.8}Co_{0.15}Mg_{0.05})O_2-(1-x)Li[Li_{1/3}Mn_{2/3}]O_2$ $(0.0 \leq x \leq 1.0)$ cathodes for Li rechargeable batteries, Solid State Sciences 12 (2010) 1797.

[16] A.D. Robertson, P.G. Bruce, Overcapacity of $Li[Ni_x Li_{1/3-2x/3}Mn_{2/3-x/3}]O_2$ electrodes, Electrochemical and Solid-State Letters 7 (2004) 294.

[17] A.R. Armstrong, A.D. Robertson, P.G. Bruce, Overcharging manganese oxides: Extracting lithium beyond Mn^{4+}, Journal of Power Sources 146 (2005) 275.

[18] C.P. Grey, W.S. Yoon, J. Reed, G. Ceder, Electrochemical activity of Li in the transition-metal sites of O_3 $Li[Li_{(1-2x)/3}Mn_{(2-x)/3}Ni_x]O_2$, Electrochemical and Solid-State Letters 7 (2004) 290.

[19] C.S. Johnson, J.S. Kim, C. Lefief, N. Li, J.T. Vaughey, M.M. Thackeray, The significance of the Li_2MnO_3 component in 'composite' $xLi_2MnO_3 \cdot (1-x)LiMn_{0.5}Ni_{0.5}O_2$ electrodes, Electrochemistry Communications 6 (2004) 1085.

[20] J.M. Zheng, X.B. Wu, Y. Yang, A comparison of preparation method on the electrochemical performance of cathode material $Li[Li_{0.2}Mn_{0.54}Ni_{0.13}Co_{0.13}]O_2$ for lithium ion battery, Electrochimica Acta 56 (2011) 3071.

[21] J.S. Cho, D.S. Jung, S.K. Hong, Y.C. Kang, Characteristics of nanosized Pb-based glass powders by high temperature spray pyrolysis method, Journal of Ceramic Society of Japan 116 (2008) 600.

[22] X. Zhang, H. Zheng, V. Battaglia, R.L. Axelbaum, Electrochemical performance of spinel $LiMn_2O_4$ cathode materials made by flame-assisted spray technology, Journal of Power Sources 196 (2011) 3640.

[23] J.H. Yi, J.H. Kim, H.Y. Koo, Y.N. Ko, Y.C. Kang, J.H. Lee, Nanosized $LiMn_2O_4$ powders prepared by flame spray pyrolysis from aqueous solution, Journal of Power Sources 196 (2011) 2858.

[24] S. Yamada, M. Fujiwara, M. Kanda, Synthesis and properties of $LiNiO_2$ as cathode material for secondary batteries, Journal of Power Sources 54 (1995) 209.

[25] T. Ohzuku, A. Ueda, M. Nagayama, Y. Iwakoshi, H. Komori, Comparative study of lithium cobalt oxide ($LiCoO_2$), lithium nickel cobalt oxide ($LiNi_{1/2}Co_{1/2}O_2$) and lithium nickel oxide ($LiNiO_2$) for 4 V secondary lithium cells, Electrochimica Acta 38 (1993) 1159.

[26] J. Morales, C. Pérez-Vicente, J.L. Tirado, Cation distribution and chemical deintercalation of lithium nickel oxide ($Li_{1-x}Ni_{1+x}O_2$), Materials Research Bulletin 25 (1990) 623.

[27] C. Delmas, M. Menetrier, L. Croguennec, S. Levasseur, J.P. Peres, C. Pouillerie, G. Prado, L. Fournes, F. Weill, Lithium batteries: a new tool in solid state chemistry, International Journal of Inorganic Materials 1 (1999) 11.

[28] Y.J. Shin, W.J. Choi, Y.S. Hong, S. Yoon, K.S. Ryu, S.H. Chang, Investigation on the microscopic features of layered oxide $Li[Ni_{1/3}Co_{1/3}Mn_{1/3}]O_2$ and their influences on the cathode properties, Solid State Ionics 177 (2006) 515.

[29] N. Yabuuchi, Y. Makimura, T. Ohzuku, Solid-State chemistry and electrochemistry of $LiCo_{1/3}Ni_{1/3}Mn_{1/3}O_2$ for advanced lithium-ion batteries,, Journal of the Electrochemical Society 154 (2007) 314.

[30] H. Xia, Y.S. Meng, M.O. Lai, L. Lu, Structural and electrochemical properties of $LiNi_{0.5}Mn_{0.5}O_2$ thin-film electrodes prepared by pulsed laser deposition, Journal of the Electrochemical Society 157 (2010) 348.

[31] S. Gopukumar, K.Y. Chung, K.B. Kim, Novel synthesis of layered $LiNi_{1/2}Mn_{1/2}O_2$ as cathode material for lithium rechargeable cells, Electrochimica Acta 49 (2004) 803.

[32] C.S. Johnson, N. Li, C. Lefief, J.T. Vaughey, M.M. Thackeray, Synthesis, characterization and electrochemistry of lithium battery electrodes: $xLi_2MnO_3 \cdot (1-x)LiMn_{0.333}Ni_{0.333}Co_{0.333}O_2$ $(0 \leq x \leq 0.7)$, Chemistry of Materials 20 (19) (2008) 6095.